SAND79-7081

MASTER

SAFEGUARDS APPLICATIONS OF FAR INFRARED RADIOMETRIC TECHNIQUES FOR THE DETECTION OF CONTRABAND

D. T. Hodges, E. E. Reber, F. B. Foote
The Aerospace Corporation

R. L. Schellenbaum, Division 1727
Sandia Laboratories

SAND79-7081
SAFEGUARDS APPLICATIONS OF FAR INFRARED RADIOMETRIC TECHNIQUES FOR THE DETECTION OF CONTRABAND

D. T. Hodges, E. E. Reber, F. B. Foote

Electronics Research Laboratory
The Aerospace Corporation
Los Angeles, California

and

R. L. Schellenbaum

Sandia Laboratories
Albuquerque, New Mexico

ABSTRACT

A new safeguards system under development employs radiometers in the 100-300 GHz spectral band to detect contraband, including shielding materials (used to attenuate the gamma ray emissions from nuclear materials), weapons, or explosives covertly concealed on personnel. Clothing is highly transparent at these frequencies and imaging techniques can detect contraband by its emissivity and reflectivity differences relative to human tissues. Experimental data are presented and sample images are used as a basis to discuss system advantages and limitations.

*This work was supported by Sandia Laboratories

SECTION I

Introduction

During the past decade, the need for new, versatile, personnel inspection techniques has arisen. Traditional systems employing magnetometers and x-ray imagers are now common in mass transportation centers, but because metal detectors are easily defeated and because x-ray imaging of personnel is prohibited by radiological health considerations, alternative or complementary approaches need to be developed In this work, a new inspection technique is investigated which utilizes radiometric imaging in the so-called far infrared (FIR), or near-millimeter-wave (NMMW), spectral region extending roughly from 300-3000 μm.[1-5] This spectral region is ideally suited for personnel inspection because the attenuation of clothing is small and because the radiation does not present a health hazard. Although the same description can apply to the microwave spectrum (3-mm to 1-cm wavelength), both the resolution for a reasonable size imaging system collection aperture and contrast between the concealed object and human tissues is degraded.[6] The FIR can provide resolution on the order of 1 cm using modest antenna apertures of 10-100 cm. Human tissue can be characterized as a nearly ideal blackbody, thus providing a uniform backdrop against which radiometric imaging and detection can be accomplished. The FIR method provides a method of material (anomoly) detection not necessarily including identification. The new detection technique creates a visual display using a cathode ray tube driven by the output of a sensitive radiometer operating in the NMMW portion of the spectrum. An optical scanning system generates a two dimensional search matrix 1 m^2 or approximately 10^4 resolution elements. It is possible to distinguish between various objects at the same absolute temperature by measuring their apparent temperature (or emissivity) with a radiometer.

Because human tissue is characterized by an emissivity close to unity at FIR/NMMW frequencies of 100 GHz (3 mm) and higher, a radiometer at these wavelengths will measure body temperatures that are roughly 10-15°C above room ambient. Concealed metallic objects will reveal themselves as regions of moderate-to-low emissivity against the uniform high emissivity background of human body tissue. These concealed objects will also shadow the radiated signal from human tissue and reflect some ambient background into the radiometer.

At the present time, radiometric detection against a human tissue background has been investigated for metallic objects, special nuclear shielding materials, and some explosives. Careful measurement of attenuation for clothing and other common concealment materials indicates only a small loss at far infrared wavelengths. Metallic objects 2 cm^2 in area were easily detected against a human backdrop with several layers of intervening clothing. The detection of nuclear shielding materials is more difficult and strongly depends on the manufacturing details of the material and the placement and contact on the subject. Explosives are very difficult to detect; however, only a small effort has been dedicated to this subject.

This paper describes the details of an FIR radiometric imaging inspection technique. Images will be used as a basis for discussing present performance and ultimate system potential.

SECTION II

Radiometry Fundamentals

All objects at temperatures above absolute zero radiate energy in the form of electromagnetic waves and absorb and reflect energy that is incident upon them. A perfect absorber is called a blackbody which is a perfect radiator and has an emission spectrum completely governed by the absolute physical temperature T. The brightness of the radiation is given by Planck's radiation law as follows:

$$B = \frac{2h\nu^3}{c^2} \quad \frac{1}{e^{h\nu/kT}-1} \qquad (1)$$

where

B = brightness (watts m^{-2} H^{-1} rad^{-2})

h = Planck's constant (6.63×10^{-34} joule-sec)

ν = frequency (Hz)

c = velocity of light (3×10^8 msec^{-1})

k = Boltzmann's constant (1.38×10^{-23} joule^{o} K^{-1})

T = temperature (^{o}K)

If Eq. (1) is integrated over all frequencies, the familiar Stefan-Boltzmann relation is obtained

$$B = \quad m^4 \qquad (2)$$

= emissivity

= constant (1.80×10^{-8} watts m^{-2}K^{-2})

In Fig. 1, several brightness curves are plotted as a function of frequency and temperature using Eq. (1). The spectral region of interest in this work includes frequencies of 100-300 GHz. In this region hν << kT so that the exponential factor in Eq. (1) is given to a good approximation by kT/hν. Thus

$$B = \frac{2\varepsilon kT}{\lambda^2} \qquad (3)$$

where λ is the wavelength in meters, and the apparent brightness is a function of the absolute temperature T and emissivity ε. Two objects at the same temperature but with different emissivities, or two identical objects at different temperatures, will radiate different amounts of energy. By using very sensitive detectors of this incoherent thermal emission it is possible to discriminate between objects at different apparent temperature ($_{\varepsilon}T$). The apparent temperature difference arises from emissivity or real absolute temperature differences. State-of-the-art detectors in the NMMW portion of the spectrum (100-300 GHz) can differentiate apparent temperature differences of a fraction of 1^{o} for a 1-sec integration time.

In radiometric systems, detection can be accomplished with the use of either coherent (heterodyne) or incoherent (video) techniques. The incoherent approach at NMMW frequencies requires liquid-helium-cooled detectors with little performance advantage relative to heterodyne detection. In the coherent approach as used in this program, the radiometer incorporates a room-temperature Schottky barrier diode mixer. The intermediate frequency (IF) is amplified by a low-noise, gallium arsenide, field-effect transistor (GaAs FET) amplifier. For a heterodyne system the minimum detectable temperature difference is given by:

$$\Delta T = \frac{T_{sys}}{(B\tau)^{\frac{1}{2}}} \qquad (4)$$

where B is the IF bandwidth, τ is the postdetection integration time, and T_{sys} is the equivalent noise temperature of the receiver.

The range of minimum detectable temperature, as a function of IF bandwidth and receiver equivalent noise temperature, is illustrated in Fig. 2. Low noise IF amplifiers are now available with frequencies up to 10 GHz, and 3000°K is a reasonable system noise temperature for receivers of 100 to 300 GHz. Temperature differentials of a fraction of a degree should therefore be readily detectable.

Passive detection systems are the most desirable because the signal is derived totally from the self-emitted radiation. However, the inspection of large areas (1 m^2) at reasonable frame rates (i.e., a few seconds) may require illumination for increased contrast. This can be accomplished using incoherent sources such as mercury arc lamps with effective brightness temperatures of a few thousand degrees in the NMMW portion of the spectrum. The UV, visible, and near-infrared emissions are filtered out so that the subject is totally unaware of the illumination and, because the flux is much less than the normal level received from the sun, the radiation hazard is negligible.[7]

SECTION III

Transmission Characteristics of Clothing and Other Common Concealment Materials

The key idea in utilizing FIR/NMMW detection and imaging is that many materials, especially clothing, become transparent in this spectral region. Visual images and infrared thermal images (thermograms) will only indicate features of the outer layers of clothing or other concealment materials.

To assess the utility of FIR/NMMW imagery, it was first necessary to investigate the transmission characteristics of materials.[1-4] Absorption coefficients are available in the literature for many materials.[8] The intent was not to repeat these careful measurements, which are generally performed on pure materials, but rather to indicate the gross transmission features of common materials which include contributions of reflection and scattering.

The transmission data are summarized in Fig. 3. As the wavelength increases beyond 1000 μm (1 mm), the transmission of even dense materials, like leather and wood, is sufficiently high to permit inspection through these materials. The data should be used as trend indicators and not for absolute numbers. The optimum region for minimum loss and maximum resolution occurs between the wavelengths of 1 and 3 mm, and actual system operating wavelength will be dictated by these conditions, the status of components, and the achievable sensitivity of detectors and radiometers.

SECTION IV

Experimental Radiometric Imaging/Detection System

The NMMW, passive imaging system, Figure 4, consists of four major subsystems; an optical-type scanning system, a radiometer for signal detection, electronics for scanning system control and signal processing, and a visual display and recording system.

The scanning system has a fixed elliptical primary mirror with focii at 1 and 3 meters. Thermal energy emitted by a body at the focus in the object plane is reflected by the vertical scan mirror, the horizontal scan mirror, the elliptical primary

mirror, and finally, into radiometer horn antenna at the image-plane focus. The scanning mirrors, therefore, sweep the 3-meter focus over the object plane while the 1-meter focus remains fixed at the radiometer.

A block diagram of the radiometer is shown in Figure 5. The thermal radiation emitted by a target is focused, through the chopper, into the radiometer horn. The radiometer is a Dicke receiver;[9] i.e., the chopper alternately blocks the signal from the target and reflects a reference signal from an ambient load into a horn antenna. The signal is squarewave-modulated at the chopper frequency, heterodyned in the mixer, amplified in the IF amplifier, and square-law detected by the diode detector. The amplitude-modulated video signal is then amplified and synchronously detected in the correlator. The resultant DC signal is integrated, amplified, and sent to the data collection system for proper display formatting. The 3-mm radiometer and imaging system has a double sideband system noise temperature of approximately 1700°K and a minimum detectable input temperature (ΔT) of approximately 0.1°K for 1-sec integration.

SECTION V

Experimental Results

The 3-mm radiometer was used to obtain single-line, horizontal scan data prior to implementation of the full scanning operation. Figure 6 shows a scan of a 2-cm-wide lead target (nuclear material shielding) against a human body with the view both unobstructed and through a 2.4-mm-thick leather jacket material. Also included is a similar scan using incoherent illumination from a mercury lamp. The detected signal is enhanced and now appears hotter than the ambient background. The results indicate that metallic objects will appear several degrees cooler in a passive detection scheme and will be detected through normal layers of clothing. As observed previously, metallic objects reflect the room ambient thermal radiation and this is compared to radiometric skin temperature. The emission temperature from the skin surface at 3 mm is approximately 295°K, and preliminary measurements at 1.4 mm indicate an emission temperature of approximately 307°K. These values vary by 2-3°K on a given subject, probably as a function of skin thickness, skin moisture, body fat layers, and other body characteristics. Typically, the emission temperature of the human body ranges from 7-10°C above ambient in the laboratory environment.

Typical passive radiometric signatures for a variety of composite shielding materials appear in Figure 7. The differential radiation, ΔT, is plotted versus real physical temperature because the latter value can vary depending on the location of the contraband sample on a human. For certain samples and physical temperatures, the differential radiance can be zero and thus the sample is radiometrically indistinguishable from the background. This ambiguity is unlikely and, in any event, can be resolved using active inspection or by comparing radiometric signatures at two wavelengths, e.g., 3 and 1.4 mm. These studies are now in progress.

Preliminary signature data for three available explosive samples (C4, detasheet, and TNT) indicate that these bare materials are difficult to detect using only passive radiometry at the 3-mm wavelength. However, explosives appear very amenable to detection using active/passive, dual wavelength radiometry, or FIR/NMMW spectral-line detection.

Imaging has also been accomplished using the system illustrated in Figure 5. The first image is designed to test spatial resolution as shown in Figure 8. The target is a variety of metallic geometric shapes, with the dimensions indicated, mounted in front of a $77^{\circ}K$ cold surface. The 3-mm image clearly indicates the presence of the smallest object (1 cm^2), although squares and circles appear the same. This is acceptable because our present goal is to detect, not necessarily identify, contraband. The data presented were recorded photographically from the display monitor without the use of image processing.

The second image (Figure 9) is the 3-mm wavelength reproduction of a handgun. The shape is readily discernible. The presence of a heavy layer of cloth over the object does not degrade the image as shown in Figure 9d.

Both of the previous figures illustrate the potential of the imaging techniques; however, the target geometry is idealized by the presence of the $77^{\circ}K$ background. Because the metal objects mask the $77^{\circ}K$ background and reflect the room ambient background, $\Delta T \approx 230^{\circ}K$. If an active imaging system were developed, the anticipated signal level would be comparable to $200^{\circ}K$. However, for passive detection, the ΔT is an order of magnitude lower and, thus is less conclusive at this point.

Figure 10 demonstrates the present prototype passive system operation for a real human subject with a concealed weapon. The weapon is detectable, but not easily identifiable, and only

relatively large objects would be seen. It will be necessary to improve the performance of the radiometer (a factor of 10 is within present capability) and to use illumination to insure large signals ($\Delta T \approx 200^{o}K$) for the detection of small (2 to 4 cm^2) objects.

SECTION VI

Conclusions

It has been demonstrated that radiometric detection of metallic objects is feasible in the 100-220 GHz band. Data obtained with a prototype, passive radiometric imaging system operating at 100 GHz indicates that target signatures (5-$10^{o}K$ ΔT and 2 cm^2 resolution) are adequate to detect contraband covertly carried by personnel - especially SNM and weapons. Clothing and other common nonmetallic materials of concealment present only a small transmission loss.

The detection of composite nuclear shielding materials is more difficult than solid materials and presents a complex set of problems that is strongly dependent on the manufacturing details of the material and the placement and contact on the subject; however, a sensitive, high-resolution scanning system should detect the object. A preliminary evaluation of explosives (C4, TNT, detasheet) at 3-mm wavelength indicates low contrast relative to human tissue background.

Radiometric improvements and illumination schemes will be implemented to increase the signal-to-noise ratio and/or inspection rate. The results to date are encouraging and work is proceeding to improve performance and address real detection scenarios.

REFERENCES

1. M. Siotto, The Use of Far-Infrared Radiation for the Detection of Concealed Metal Objects, DOT-TSC-OST-72-11, U. S. Department of Transportation, Washington, D.C. (November 1971).

2. J. E. Robinson, "The Use of InSb Free Electron Bolometers in a Submillimeter Imaging System," in Proceedings of the IRIS Meeting of Specialty Group on Infrared Detectors, March 1973, pp. 23-31.

3. D. H. Barker, D. T. Hodges, T. S. Hartwick, "Far Infrared Imagery," SPIE J. 67 27-34 (1975).

4. T. S. Hartwick, D. T. Hodges, D. H. Barker, and F. B. Foote, "Far Infrared Imagery," Appl. Opt. 15, 1919-1921 (1976).

5. T. S. Hartwick, "Far Infrared Imaging for Law Enforcement Applications," SPIE J. 108, 139-140 (1977).

6. R. M. Weigand, A Microwave Technique for Detecting and Locating Concealed Weapons, DOT-TSC-OST-72-15, U. S. Department of Transportation, Washington, D.C. (December 1971).

7. H. P. Schwan, and K. Li, "Hazards Due to Total Body Irradiation by Radar," Proc. IRE, Vol. 44, P. 1572 (November 1956).

8. K. D. Moller and W. G. Rothschild, Far Infrared Spectroscopy (Wiley-Interscience, New York, 1971).

9. J. D. Krans, Radio Astronomy (McGraw Hill, San Francisco, 1966).

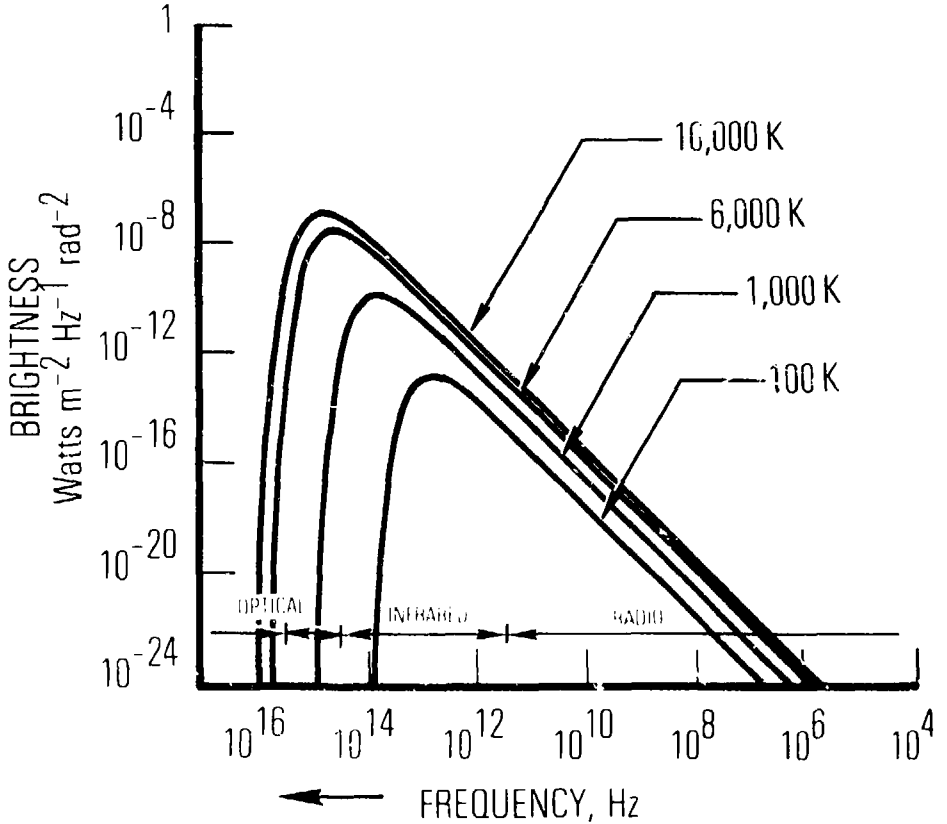

Spectral brightness curves showing [illegible] general blackbodies of the temperatures indicated.

FIGURE 2

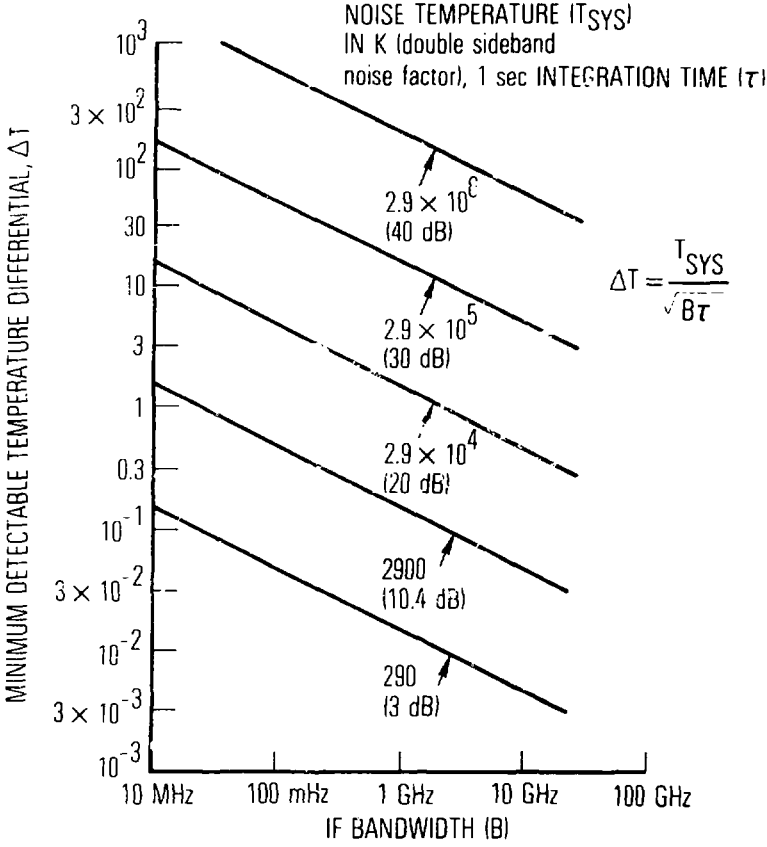

Theoretical performance of coherent radiometer, 1-second integration time. The parametric curves indicate system noise temperatures of the radiometer receiver.

FIGURE 3

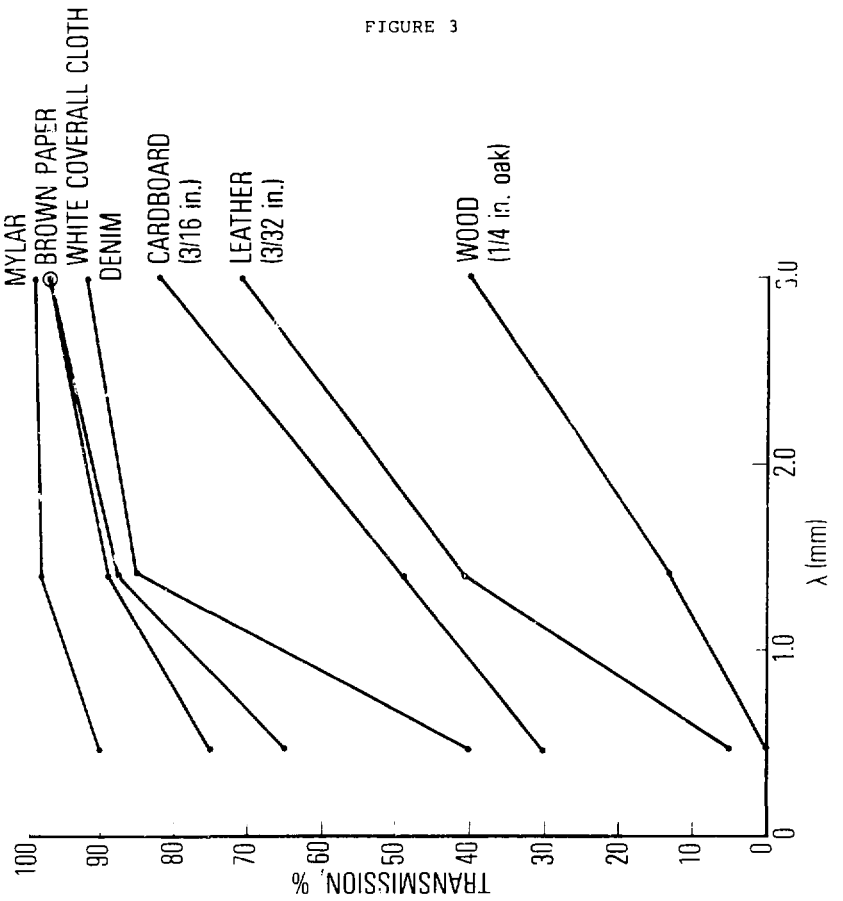

Transmission of representative concealment materials in the FIR-NMMW spectral region. Losses include the effects of absorption, reflection, and scattering.

FIGURE 4

NMMW passive imaging system block diagram

FIGURE 5

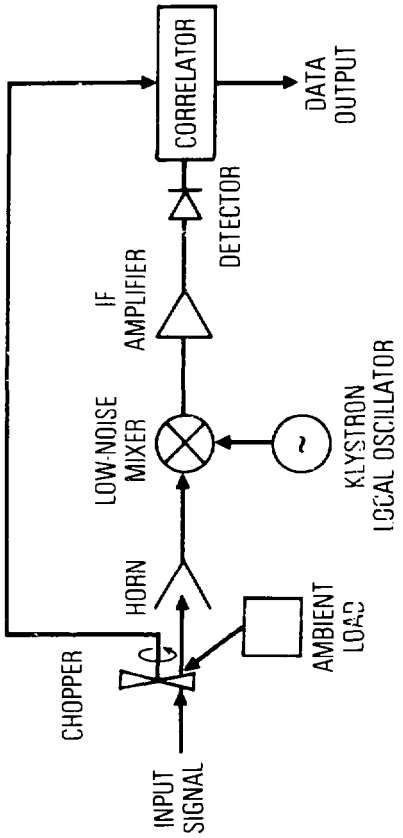

Radiometer Block Diagram

FIGURE 6

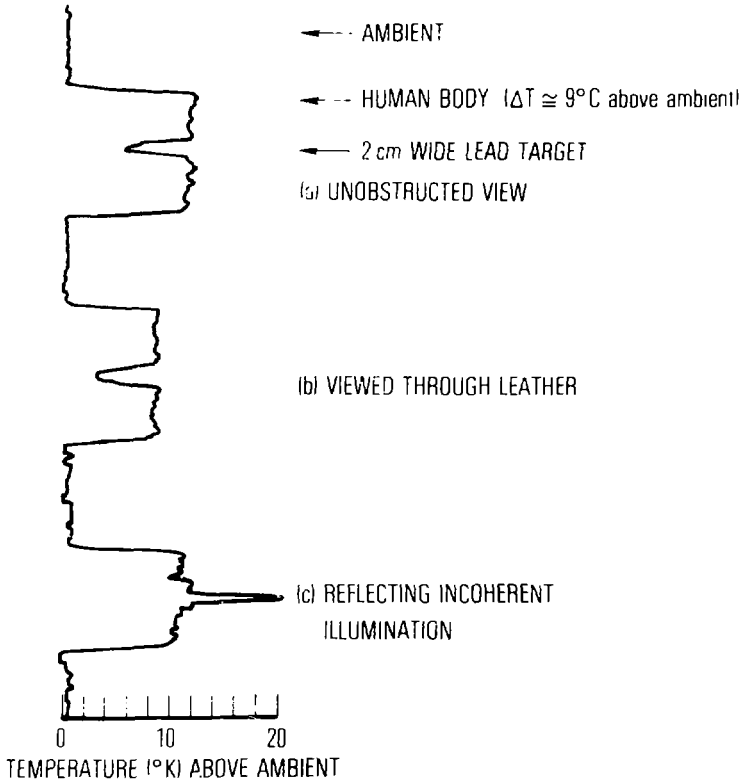

3-mm radiometric scan of 2-cm wide lead target against a human body.

FIGURE 7

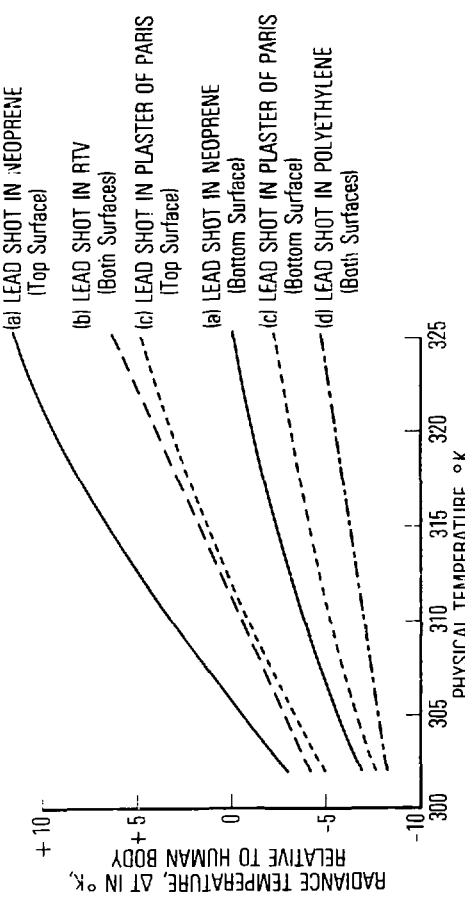

3-mm radiance temperature versus physical temperature of composite shielding materials.

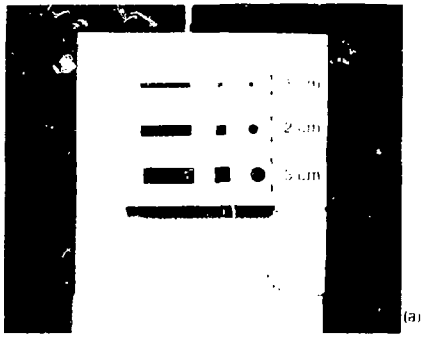

(a)

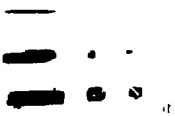

(b)

(c)

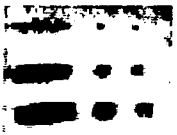

(d)

Images in the visible and at the 3-mm wavelength of 1-, 2-, and 3-cm metal objects.

(a) Photograph of objects in front of liquid-nitrogen-cooled background (77 K).

(b) 3-mm image.

(c) Photograph of objects covered with heavy black cloth.

(d) 3-mm image of covered objects.

FIGURE 9

Images in the visible and at the 3-mm wavelength of a Smith & Wesson .38 special revolver.

(a) Photograph of revolver in front of liquid-nitrogen-cooled background (77°K).

(b) 3-mm image.

(c) Photograph of revolver covered with heavy black cloth.

(d) 3-mm image of covered revolver.

[illegible] and at the 3-mm wavelength [illegible] common .38 special revolver on a human [illegible] shot graphs on left with corresponding [illegible].